Franklin, R. E. (1955) *Nature (London) 175*, 379–381.
Franklin, R. E. (1956) *Biochim. Biophys. Acta 19*, 203–211.
Hirth, L., & Richards, K. E. (1981) *Adv. Virus Res. 26*, 145–199.
Lomonossoff, G. P., & Wilson, T. M. A. (1985) *Molecular Plant Virology* (Davies, J. W., Ed.) Vol. I, pp 43–83, CRC Press, Boca Raton, FL.
Namba, K., & Stubbs, G. (1986) *Science (Washington, D.C.) 231*, 1401–1406.
Nonomura, Y., & Ohno, T. (1974) *J. Mol. Biol. 90*, 523–527.
Potschka, M. (1983) Ph.D. Thesis, University of Vienna.
Raghavendra, K., Adams, M. L., & Schuster, T. M. (1985) *Biochemistry 24*, 3298–3304.
Schuster, T. M., Scheele, R. B., & Khairallah, L. H. (1979) *J. Mol. Biol. 127*, 461–486.
Schuster, T. M., Scheele, R. B., Adams, M. L., Shire, S. J., Steckert, J. J., & Potschka, M. (1980) *Biophys. J. 32*, 313–329.
Shire, S. J., Steckert, J. J., Adams, M. L., & Schuster, T. M. (1979a) *Proc. Natl. Acad. Sci. U.S.A. 76*, 2745–2749.
Shire, S. J., Steckert, J. J., & Schuster, T. M. (1979b) *J. Mol. Biol. 127*, 487–506.
Steckert, J. J. (1982) Ph.D. Thesis, University of Connecticut.
Steckert, J. J., & Schuster, T. M. (1982) *Nature (London) 299*, 32–36.
Stubbs, G. (1984) *Biological Macromolecules and Assemblies* (Jurnak, F. A., & McPherson, A., Eds.) Vol. 1, pp 149–202, Wiley, New York.
Stubbs, G., Warren, S., & Holmes, K. (1977) *Nature (London) 267*, 216–221.
Unwin, P. N. T., & Klug, A. (1974) *J. Mol. Biol. 87*, 641–656.
Vogel, D. (1982) *Biochim. Biophys. Acta 706*, 65–79.

Calcium–Proton and Calcium–Magnesium Antagonisms in Calmodulin: Microcalorimetric and Potentiometric Analyses†

Mladen Milos,‡ Jean-Jacques Schaer,‡ Michelle Comte,§ and Jos A. Cox*,§
Department of Physical Chemistry and Department of Biochemistry, University of Geneva, Geneva, Switzerland
Received January 31, 1986; Revised Manuscript Received May 2, 1986

ABSTRACT: Microcalorimetry, pH potentiometry, and direct binding studies by equilibrium dialysis or gel filtration were performed to determine the thermodynamic functions $\Delta H°$, $\Delta G°$, and $\Delta S°$ guiding the interactions of Ca^{2+}, Mg^{2+}, and H^+ with bovine brain calmodulin. At pH 7.5, Ca^{2+} and Mg^{2+} binding are both endothermic with enthalpy changes of 19.5 and 72.8 kJ·(mol of calmodulin)$^{-1}$, respectively. These enthalpy changes are identical for each of the four ion-binding domains. The affinity constants also are identical with intrinsic values of 10^5 M^{-1} for Ca^{2+} and 140 M^{-1} for Mg^{2+}. Ca^{2+} and Mg^{2+} do not compete for the same binding sites: at high concentrations of both ions, a calmodulin–Ca_4–Mg_4 species is formed with an enthalpy value of 24.4 kJ·mol^{-1} with respect to calmodulin–Ca_4 and −28.8 kJ·mol^{-1} with respect to calmodulin–Mg_4. Moreover, in the presence of high concentrations of Ca^{2+}, the affinity of each of the four ion-binding domains in calmodulin for Mg^{2+} is decreased by a factor of 4 and vice versa, indicative of negative free-energy coupling between Ca^{2+} and Mg^{2+} binding. Protons antagonize Ca^{2+} and Mg^{2+} binding in a different manner. Ca^{2+}–H^+ antagonism is identical in each of the four Ca^{2+}-binding domains in the pH range 7.5–5.2. Our analyses suggest that three chemical geometries, probably carboxyl–carboxylate interactions, are responsible for this antagonism with ionization constants of $10^{6.2}$ M^{-1} in the metal-free protein. Mg^{2+}–H^+ antagonism also is identical for each of the Mg^{2+}-binding sites but is qualitatively different from Ca^{2+}–H^+ antagonism. The localization of the putative Mg^{2+}-binding sites and the structural basis of the Ca^{2+}–H^+ antagonism have been discussed.

In eukaryotic cells, calmodulin (CaM)[1] is a vector in the stimulus-response coupling since it is sensitive to raised [Ca^{2+}] and subsequently activates a number of enzymes. Since activation is critically dependent on the number of Ca^{2+} ions bound to the vector [for review, see Cox (1984)], it is of crucial importance to know in detail the characteristics of Ca^{2+} binding to the latter and the influence, even small, of other ions present in the cell. Unfortunately, controversy exists regarding the affinities of the four Ca^{2+}-binding domains, the cooperativity in binding, and the influence of Mg^{2+} and monovalent cations on Ca^{2+} binding. Seven different groups [mentioned by Burger et al. (1984); also Ogawa and Tanokura (1984)], who performed direct binding studies in buffers of sufficient ionic strength to eliminate electrostatic effects (Debye & Hückel, 1923), experienced that the shape of the binding isotherm is close to the ideal Langmuir isotherm, which led us to assume a simple model of four independent Ca^{2+}-binding sites of equal affinity (Burger et al., 1984). However, from studies using ^{43}Ca NMR (Andersson et al., 1982) and fast kinetics of Ca^{2+} off-rates (Bayley et al., 1984), it appears that CaM contains two low- and two high-affinity pairs of sites

† This work was supported by Swiss NSF Grant 3.161.0.85 and by the Muscular Dystrophy Association of America, Inc.
* Author to whom correspondence should be addressed.
‡ Department of Physical Chemistry.
§ Department of Biochemistry.

[1] Abbreviations: CaM, calmodulin; EGTA, ethylene glycol bis(β-aminoethyl ether)-*N,N,N',N'*-tetraacetic acid; PIPES, 1,4-piperazinediethanesulfonic acid.

0006-2960/86/0425-6279$01.50/0

with a 40–70-fold difference in the binding constants. Recently, Martin et al. (1985) reported that upon increasing the ionic strength to physiological levels the differences in affinity are reduced to 1 order. Assuming a 1 order difference, Wang (1985) proposed an elegant theoretical explanation of the discrepancies between the above two lines of studies, but the strong positive cooperativity of Ca^{2+} binding in both halves of CaM, postulated by the author, is not evident, at least for the N-terminal pair of domains (Minowa & Yagi, 1984). Furthermore, by direct binding experiments on tryptic fragment of CaM, Minowa and Yagi (1984) found only a 3-fold difference in the affinities of the N- and C-terminal halves.

Another controversial point is the effect of Mg^{2+} on Ca^{2+} binding. Two well-documented direct binding studies (Haiech et al., 1981; Ogawa & Tanokura, 1984) indicate that there is straight competition of Ca^{2+} and Mg^{2+} for the same four binding sites with affinity constants for Mg^{2+} of 130–300 M^{-1} when the total ionic strength in the experiment is reasonably high (>0.1 M). However, other authors did not observe such pronounced competition effects at millimolar free Mg^{2+} concentrations (Potter et al., 1981; Cox et al., 1981; Burger et al., 1984). As for the specific effect of monovalent cations on Ca^{2+} binding forwarded by Haiech et al. (1981), Ogawa and Tanokura (1984) considered it as an effect of ionic strength, which logically must play a significant role in this type of interaction [for review, see Cox et al. (1984)].

More fundamental parameters than the binding constants of metal ion interaction with CaM are the changes in enthalpy and entropy of the equilibrium reactions. Using microcalorimetry, Tanokura and Yamada (1984) measured at 25 °C two different endothermic enthalpy components when Ca^{2+} binds to the two pairs of sites and a 25-fold difference in affinity for Ca^{2+}. In the presence of 5 mM Mg^{2+}, these enthalpy changes are exothermic with a 60-fold difference in affinity. It should be noted that at the high concentrations of CaM used the precision in the determination of the affinity constants is very poor (errors in the log K values are estimated at ±0.5 according to the authors) and that as a mean only three Ca^{2+}-binding sites were titrated. Furthermore, their study did not include a schematic description of the Ca^{2+}–Mg^{2+} antagonism and lacks internal consistency in the competition data. Here we present a refined microcalorimetric investigation of Ca^{2+} and Mg^{2+} binding to CaM and of the Ca^{2+}–Mg^{2+} antagonism, as well as direct binding studies on the antagonism Ca^{2+}–Mg^{2+}, Ca^{2+}–H^+, and Mg^{2+}–H^+ in CaM.

Materials and Methods

Protein and Protein Concentration. Bovine brain CaM was purified by affinity chromatography on phenyl-Sepharose according to the method described by Gopalakrishna and Anderson (1982) followed by hydroxylapatite chromatography (Wallace & Cheung, 1979). The protein concentration was determined on the metal-free sample (see below) and also on the protein that contains exclusively Mg^{2+} with a specific extinction coefficient of $A^{1\%}_{277nm} = 1.80$ and on Ca^{2+}-containing CaM with $A^{1\%}_{275nm} = 1.71$. The molar concentrations were calculated with a M_r of 16737 for metal-free CaM (taken from the amino acid sequence; Wada et al., 1985).

Metal Ion Determination and Metal Removal from CaM. Total Ca^{2+} and Mg^{2+} concentrations were measured by flame photometry with a Perkin-Elmer 2380 atomic absorption spectrophotometer using Titrisol standards diluted in the assay buffers. To minimize quenching, 1 mM EDTA was usually added to the samples and the standards. The assay buffers were routinely passed over Chelex X-100 to reduce the contamination by Ca^{2+}. Ca^{2+} removal from CaM and equilibration in the assay buffer was as follows: to ca. 100 mg of CaM in 10 mL of 50 mM Tris-HCl, pH 7.5 and 3 mM EDTA ammonium sulfate suprapure (Merck, Darmstadt, West Germany) was added to a final saturation of 95%. After centrifugation at 50000g for 15 min, the precipitate was washed twice with 16 mL of saturated ammonium sulfate and 3 mM EDTA. Subsequently, the precipitate was washed in 16 mL of saturated ammonium sulfate without EDTA, brought to pH 3.9 with acetic acid. The pellet was dissolved in 2 mL of 50 mM PIPES buffer, pH 7.5, and chromatographed on a column (1 × 50 cm) of Sephadex G-25, equilibrated in the desired buffer. Using this method, we did not experience problems with the UV absorption spectrum (the 259 to 277 nm ratio was typically 0.79 ± 0.01 for all our CaM samples used) and with the determination of the protein concentration. Ca^{2+} contamination was always less than 0.02 mol·(mol of protein)$^{-1}$ (0.5% of the Ca^{2+}-binding capacity) and often as low as 0.005 mol·(mol of CaM)$^{-1}$.

Direct Divalent Cation Binding. Direct Ca^{2+}-binding experiments were carried out in 50 mM PIPES buffer, pH 5.8 or 5.0, and 150 mM NaCl at 25 °C, as previously described (Burger et al., 1984). Increments of $CaCl_2$ were added to 170 μM metal-free CaM while the free Ca^{2+} concentrations were measured with a Philips 561 Ca^{2+}-selective electrode. The latter was standardized with Titrisol–Ca^{2+} solutions diluted in the assay buffer. Regularly during the titration, aliquots were withdrawn to check the total Ca^{2+} concentration by flame photometry. Some equilibrium dialysis experiments, carried out as previously described (Burger et al., 1984), completed the electrode method. Direct Mg^{2+}-binding experiments were carried out at 25 °C by the Hummel–Dryer gel filtration technique (Burger et al., 1983) on a 50 × 0.9 cm column of Sephadex G-25 equilibrated in 50 mM PIPES–NaOH, pH 7.5, 150 mM NaCl, and the indicated concentrations of $MgCl_2$ and/or $CaCl_2$. A total of 100 mg of CaM in 2 ml of buffer was applied to the column and eluted at a rate of 100 μL·min^{-1}.

Proton Release. Proton release was monitored in either of two ways: directly by pH potentiometry or indirectly by microcalorimetry. In the first method, 5 mL of 300 μM metal-free CaM in 150 mM KCl was installed in a pH-stat assembly of Radiometer titrator 11, equipped with an autoburette ABU 13, and flushed for 30 min with nitrogen. Subsequently, the proton release upon addition of increments of $CaCl_2$ or $MgCl_2$ was measured at an imposed pH by back-titration of the protein solution with 10 mM NaOH (Titrisol, Merck). After each increment, a small aliquot was withdrawn for determination of the total Ca^{2+} or Mg^{2+} concentrations. Blank experiments without protein were carried out at each pH in order to perform the necessary small corrections.

Proton release was also measured by microcalorimetry either at pH 7.5 with Tris and PIPES buffer or at pH 5.3 with acetate and histidine as buffers. Since at each pH the same reaction was monitored in the two buffers, the difference in heat production or absorption is due to the difference in protonation of the buffer only. The standard enthalpy changes of protonation of Tris and PIPES are −47.53 and −11.46 kJ·mol^{-1}, respectively (Beres & Sturtevant, 1971); that of histidine is −29.30 kJ·mol^{-1} (Martell & Smith, 1974) and that of acetate 0.42 kJ·mol^{-1} (Martell & Smith, 1977a).

Microcalorimetry. Enthalpy changes were determined in an LKB 2277 flow microcalorimeter (Schaer et al., 1985) at 25.0 ± 0.1 °C. A 32–400 μM stock solution of metal-free CaM in the desired buffer and varying concentrations of $CaCl_2$ or $MgCl_2$ in the same buffer were introduced at equal flow

rates in the mixing chamber of the microcalorimeter by means of a two-channel peristaltic pump at a total rate of 9 $mL \cdot h^{-1}$. The observed thermal effects were calibrated by electrical simulation. For each concentration studied, the heat of dilution of Ca^{2+} and Mg^{2+} was corrected for by adjusting the base line to zero before protein injection. In all figures except Figure 2, the noise-to-signal ratio was at the utmost 0.03.

Data Treatment. Since proton and enthalpy titrations were monitored with CaM concentrations of 16–300 μM and the affinity constant for Ca^{2+} is about 10^5 M^{-1} (much lower even for Mg^{2+}, see below), not all added Ca^{2+} or Mg^{2+} can be considered as bound to the protein. Assuming identical affinity constants (K_M), a limited number of binding sites, and an identical signal change (ΔY) for each of the sites, the titration data can be described by eq 3 and 5 of the Appendix. When two pairs of different affinity are postulated, the titration data have to be described by eq 4 and 5 of the Appendix. In the case of Ca^{2+} binding, the 4:1 stoichiometry can easily be observed graphically (Figures 1 and 3), and therefore, the total concentration of metal ion sites (S_T) was taken as 4 times the total CaM concentration ($[CaM_T]$). In the case of Mg^{2+} binding, the stoichiometry could not be established from the titration data since the amount of bound Mg^{2+} is negligible when compared to the amount of added Mg^{2+}. On the basis of conclusions from direct binding experiments (see Results), S_T was set equal to 4 times the total CaM concentration for the computations.

In this study, the binding of two ligands, A and B, to a protein metal ion binding site (S) involved negative free-energy coupling according to Scheme I. In Scheme I, K_a and K_b are the association constants for A and B, respectively, in the absence of the other ligand, and K_a^b and K_b^a the corresponding constants in the presence of infinite concentrations of the second ligand. The amount of bound ligand per mole of site was calculated with eq 9 and 10 of the Appendix.

Scheme I

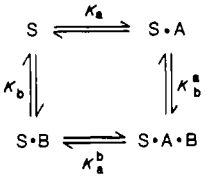

RESULTS

Enthalpy Titration of CaM–Ca^{2+} Interaction. Figure 1A shows the evolution of heat absorption upon increasing the ratio of $Ca^{2+}{}_T$ per CaM in 50 mM PIPES, pH 7.5, and 150 mM NaCl or 150 mM KCl at 25 °C. As already mentioned by Tanokura and Yamada (1984), who worked at pH 7.0 in 20 mM PIPES and 150 mM KCl, Ca^{2+} binding to CaM is endothermic, but in contrast to their observations, the titration profile was close to linear up to a ratio of ca 3.0 mol of $Ca^{2+} \cdot (\text{mol of protein})^{-1}$. When high concentrations of CaM were used, hence of metal-binding sites ($S_T \gg 1/K_{Ca}$), the enthalpy titration curve is essentially stoichiometric and does not depend on the affinity constants. Figure 2 shows that in an experiment with 200 μM CaM (after mixing) binding of the third and fourth Ca^{2+} produces the same enthalpy variation as binding of the first or of the second Ca^{2+}. Hence, it can reasonably be concluded that the $\Delta H°$ values are identical for the four Ca^{2+}-binding domains. In the light of the controversy about the affinity of CaM for Ca^{2+} (resumed in the introduction), we chose to perform also an enthalpy titration at a concentration of CaM that is optimal to distinguish between the model of four identical sites with K_{Ca} equal to 10^5 M^{-1} and

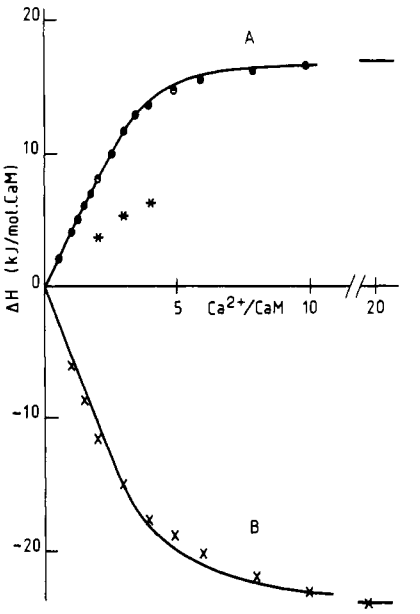

FIGURE 1: Enthalpy titration profile of Ca^{2+} binding to CaM in the absence (A) or presence (B) of 30 mM $MgCl_2$. CaM concentration after mixing was 50 μM. All experiments were carried out in 50 mM PIPES–NaOH, pH 7.5, and 150 mM NaCl, except for the following: (*) 50 mM Tris, pH 7.5, 150 mM NaCl; (O) 50 mM PIPES–KOH, pH 7.5, 150 mM KCl. The solid curves and the plateau values were calculated with eq 3 and 5 of the Appendix. The best fitting parameters are $\Delta G° = 17.0$ $kJ \cdot mol^{-1}$ and $K_{Ca} = 1.3 \times 10^5$ M^{-1} in the absence of Mg^{2+} and $\Delta H° = -24.0$ $kJ \cdot mol^{-1}$ and $K_{Ca}(app) = 7.2 \times 10^4$ M^{-1} in the presence of 30 mM $MgCl_2$.

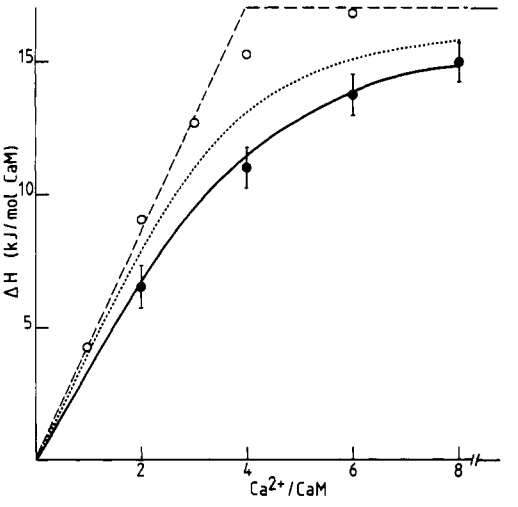

FIGURE 2: Enthalpy titration of Ca^{2+} binding to CaM at high or low protein concentration in 50 mM PIPES–NaOH, pH 7.5, and 150 mM NaCl. CaM concentration after mixing was 200 (O) or 16 μM (●). The vertical bars indicate the noise amplitude. The solid line was calculated with eq 3 and 5 of the Appendix by assuming four identical affinity constants equal to 10^5 M^{-1}; the dotted line was calculated with eq 4 and 5 of the Appendix by assuming two pairs of sites with $K_M = 10^6$ M^{-1} for one pair and 10^5 M^{-1} for the other. In both cases the $\Delta H°$ value was 17.0 $kJ \cdot mol^{-1}$. The dashed line represents the stoichiometric titration (with infinite $[CaM_T]$).

the model of two pairs of sites with different affinities [two sites with $K_{Ca} = 10^6$ M^{-1} and two with $K_{Ca} = 10^5$ M^{-1}; see Wang (1985) and references cited therein]. Figure 2 shows that at 16 μM CaM (after mixing) the experimental data are clearly in favor of the first model, thus confirming a more extensive study from our laboratory (Burger et al., 1984). This statement is strengthened by the fact that the enthalpy titration profile at 50 μM CaM (Figure 1A) fitted well with eq 3 and 5 of the Appendix, assuming four identical affinity constants

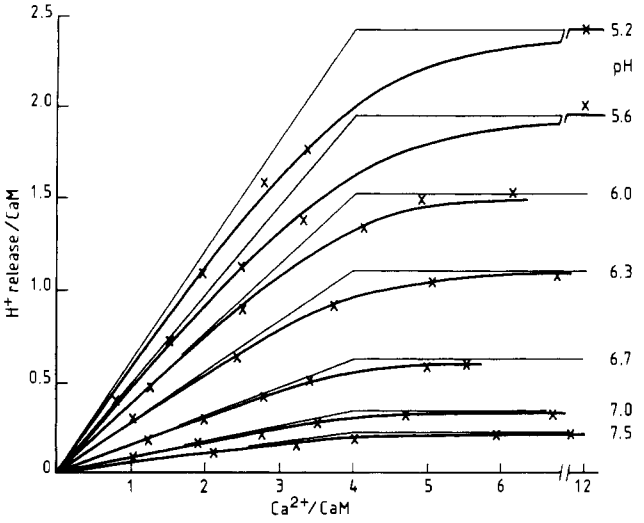

FIGURE 3: Proton release at different constant pH values upon Ca^{2+} binding to CaM (×). Concentration of protein was 260–300 μM. The thick solid curves represent the best fit of the experimental data with eq 3 and 5 of the Appendix, with the following apparent K_{Ca} values: 1.02×10^5 for pH 7.5; 9.7×10^4 for pH 7.0; 6.5×10^4 for pH 6.7; 5.3×10^4 for pH 6.3; 3.8×10^4 for pH 6.0; 2.8×10^4 for pH 5.6; 1.8×10^4 for pH 5.2. The thin lines represent true stoichiometric titrations (with infinite $[CaM_T]$) calculated from the values deduced from eq 3 and 5 of the Appendix.

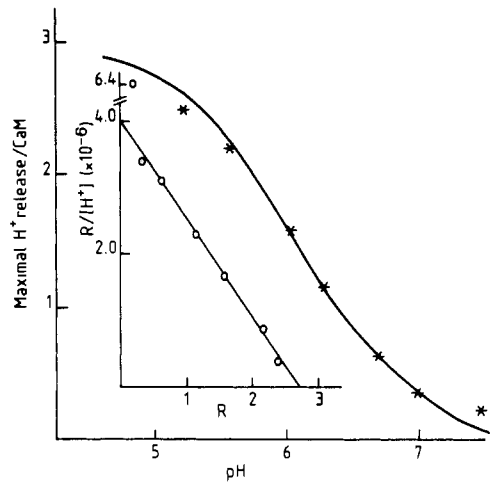

FIGURE 4: Maximal proton release upon binding of four Ca^{2+} (taken from Figure 3) as a function of pH and corresponding Scatchard plot (inset). R = maximal proton release per mole of CaM.

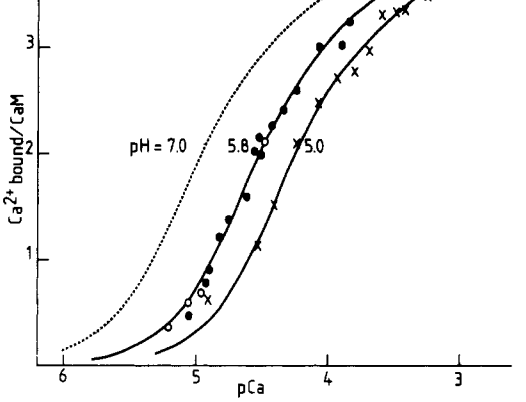

FIGURE 5: Direct Ca^{2+} binding to CaM in 50 mM PIPES–150 mM NaCl at pH 5.8 (●, ○) and pH 5.0 (×). All measurements were carried out with the Ca^{2+}-selective electrode, except four points at pH 5.8 (○), which represent equilibrium dialysis experiments. The theoretical isotherm at pH 7.0 was taken from Burger et al. (1984).

and identical enthalpy changes for the four Ca^{2+}-binding sites. The calculated parameters are $\Delta H^\circ = 17.0 \pm 0.3$ kJ·mol^{-1} for binding of four Ca^{2+} and $K_{Ca} = 1.3 \times 10^5$ M^{-1}. The latter value compares fairly well with the affinity constant of 9.3×10^4 M^{-1} reported previously (Burger et al., 1984).

The total enthalpy change has to be corrected for the heat resulting from neutralization by PIPES buffer of protons released upon Ca^{2+} binding. The latter was determined by complementary microcalorimetric measurements in Tris-HCl [Figure 1A (*)] as described under Materials and Methods and amounts of 0.27 proton upon binding of four Ca^{2+} per mole of CaM. The corrected enthalpy change for binding of four Ca^{2+} is thus 19.5 kJ·mol^{-1}. Figure 1A also shows that replacement of Na^+ ions by K^+ under otherwise identical ionic conditions does not change the enthalpy values of Ca^{2+} binding, suggesting that a nonspecific ionic strength effect, rather than competition between K^+ and Ca^{2+}, explains in a satisfactory way the experimental data.

Ca^{2+}–H^+ Antagonism in CaM. Since proton antagonism in Ca^{2+} binding to CaM is suggested from the data of Haiech et al. (1981) and from proton release upon Ca^{2+} binding at pH 7.5 (see above), we studied this phenomenon by titration of proton release upon Ca^{2+} binding at different pH values and also by direct binding studies. Figures 3 shows that the experimental titration curves, especially at pH ≥6.0, are close to real stoichiometric titrations (thin lines) with a break at 4 mol of Ca^{2+} added per mole of protein and that the data fit with eq 3 (thick lines). Hence, at all the pH values studied, proton release is proportional to Ca^{2+} binding for all the four Ca^{2+}-binding sites. Proton release is maximal around pH 5.0 and nearly negligible at pH 7.5. Figure 4 shows that the chemical configurations responsible for H^+ release are very homogeneous with respect to their apparent ionization constants, $pK_i = 6.17$, and that 2.7 protons are released when CaM binds four Ca^{2+} ions. The Ca^{2+}-dependent proton release at pH 5.3 was verified by an independent method, i.e., microcalorimetry in two buffers of different protonation enthalpy. Table I shows that at this pH proton release is strictly proportional to the amount of bound CaM at saturation values of 1.3, 2.4, or 3.1 mol of Ca^{2+} per mole of CaM. The amount released, 2.08 mol of H^+, was somewhat lower than that found by direct pH-stat titration, i.e., 2.3 mol of H^+ at pH 5.3

Table I: Proton Release upon Ca^{2+} or Mg^{2+} Binding Measured by Microcalorimetry in 50 mM Histidine or Acetate Buffer, pH 5.3, and 150 mM NaCl[a]

total $[M^{2+}]$ after mixing	fractional saturation[b]	kJ·(mol of CaM)$^{-1}$		ΔH^+ released per CaM[d]	maximal H^+ released[e]
		ΔH_{Ac}[c]	ΔH_{His}[c]		
Ca^{2+}					
80 μM	0.29	6.67	−11.45	0.61	2.12
160 μM	0.51	11.92	−21.46	1.12	2.19
250 μM	0.67	13.75	−25.28	1.31	1.94
Mg^{2+}					
7.5 mM	0.51	36.96	0	1.24	2.45
15 mM	0.67	46.08	−1.44	1.60	2.37
30 mM	0.81	58.08	−2.88	2.05	2.54

[a] CaM concentration after mixing 50 μM. [b] Calculated using $K_{Ca} = 1.8 \times 10^4$ M^{-1} (taken from Figure 3) and $K_{Mg} = 140$ M^{-1} (taken from Figure 6). [c] ΔH_{Ac} is the measured enthalpy change in acetate buffer; ΔH_{His} is the one in histidine buffer. [d] The number of protons released equals $(\Delta H_{Ac} - \Delta H_{His})/29.71$ kJ with 29.71 kJ being the difference in protonation enthalpy of the acetate and histidine buffer (0.42 + 29.29 kJ). [e] Maximal proton release stands for the number of protons released at pH 5.3 upon saturation of CaM by Ca^{2+} and is calculated by dividing values of the preceding column by the fractional saturation.

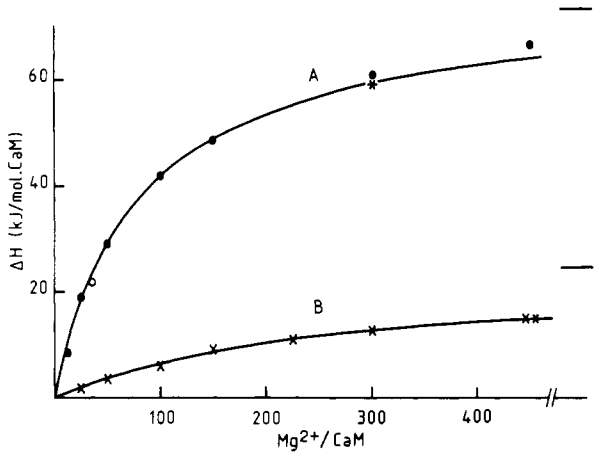

FIGURE 6: Enthalpy titration profile of Mg^{2+} binding to CaM in the absence (A) or presence (B) of 1 mM $CaCl_2$. CaM concentration after mixing was 100 μM. All experiments were carried out in 50 mM PIPES–NaOH, pH 7.5, and 150 mM NaCl, except for the following: (*) 50 mM Tris, pH 7.5, 150 mM NaCl; (O) 50 mM PIPES–KOH, pH 7.5, 150 mM KCl. The solid curves and the plateau values were calculated from the experimental data with eq 3 and 5 of the Appendix. The best fitting parameters are ΔH° = 72.8 kJ·mol^{-1} and K_{Mg} = 140 M^{-1} in the absence of $CaCl_2$ and ΔH° = 24.4 kJ·mol^{-1} and K_{Mg}(app) = 35 M^{-1} in the presence of 1 mM $CaCl_2$.

(Figure 4). It should be noted that the estimation by microcalorimetry is more prone to inaccuracy.

Since direct Ca^{2+}-binding studies were carried out in the relevant pH range (Figure 5). At both pH 5.0 and 5.8, CaM binds four Ca^{2+}, but the curves are gradually shifted to higher [Ca^{2+}] values upon increasing the proton concentration without much of a shape change when compared to the isotherm at pH 7.0. Hence, the decrease in affinity takes place to the same extent for each of the binding sites.

Enthalpy Titration of CaM–Mg^{2+} Interaction. Figure 6 shows the enthalpy titration profile of Mg^{2+} interaction with CaM in the absence of Ca^{2+}. As with Ca^{2+}, the binding of Mg^{2+} to CaM is an endothermic process, but saturation proceeds slowly upon addition of Mg^{2+}, so that during the whole titration CaM-bound Mg^{2+} is negligible as compared to the free concentration of Mg^{2+}. Iterative fitting of the experimental data according to eq 3 and 5 (model 1) of the Appendix yields the following parameters: K_{app} for Mg^{2+} is 140 M^{-1} and ΔH° is 72.8 kJ·(mol of protein)$^{-1}$. In this data treatment, the ϕ^2 value—defined as equal to $\sum_{i=1}^{i=n}(\Delta Y_{exptl} - \Delta Y_{calcd})^2/(0.05\Delta Y_{exptl})$; see Burger et al. (1984)—equals 1.20. When we assume model 2, i.e., two pairs of sites with a difference in affinity constants of 1 order, the iterative fitting yielded the following values: K_1 = 422 M^{-1}; K_2 = 46 M^{-1}; ΔH°_{max} = 72.8; ϕ^2 = 46.97. Complementary microcalorimetric experiments of Mg^{2+} binding in Tris-HCl buffer (Figure 6) at pH 7.5 revealed that binding of this ion does not lead to measurable proton release, so that no correction needed to be made for the enthalpy change. The enthalpy titration profile of Figure 6 does not allow the determination of the stoichiometry of Mg^{2+} binding to CaM. We therefore performed direct binding experiments, using the Hummel–Dryer gel filtration technique (Burger et al., 1983) with high amounts of CaM at submicromolar concentrations of free Ca^{2+}. The raw data are similar to those illustrated for Mg^{2+} binding in the presence of millimolar free Ca^{2+} (see below). The Scatchard plot (Figure 7) of five experiments shows that 4.75 mol of Mg^{2+} can be bound to 1 mol of CaM with an affinity constant of 174 M^{-1}. The latter value is very similar to the one obtained by microcalorimetry and confirms that the Mg^{2+}-specific sites have all the same affinity. It should be noted that two equilibrium

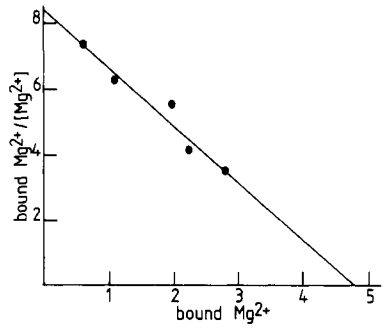

FIGURE 7: Scatchard plot of Mg^{2+} binding to CaM in the absence of $CaCl_2$ as determined by Hummel–Dryer equilibrium gel filtration experiments.

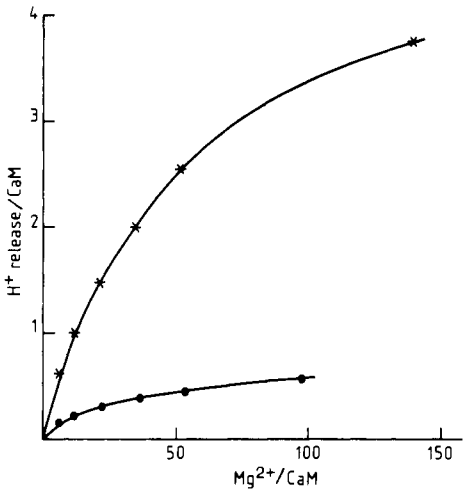

FIGURE 8: Proton release at pH 6.0 (●) and pH 5.0 (*) upon Mg^{2+} binding to CaM. Concentration of protein was 250–300 μM. The solid curves represent the best fits of the experimental points with eq 3 and 5 of the Appendix with ΔY_{max} of 0.66 and 5.3 H^+ per mole of CaM and K_{Mg} of 167 and 72 M^{-1}, respectively.

Table II: Stoichiometry of Mg^{2+} and Ca^{2+} Binding to CaM As Determined by Equilibrium Gel Filtration

free divalent ion concn	per mol of CaM	
	bound Mg^{2+}	bound Ca^{2+}
5.0 mM Mg^{2+}, 1.0 mM Ca^{2+}	0.80	3.69
5.6 mM Mg^{2+}, 2.2 mM Ca^{2+}	0.84	4.52
8.1 mM Mg^{2+}, 1.2 mM Ca^{2+}	1.05	3.98
9.3 mM Mg^{2+}, 2.5 mM Ca^{2+}	1.55	3.71

filtration experiments above 10 mM free Mg^{2+} yielded data that do not fit in the Scatchard plot: at 11.5 and 17.8 mM free Mg^{2+}, the extent of Mg^{2+} binding was 4.1 and 6.1 mol·(mol of CaM)$^{-1}$, respectively. Clearly, nonspecific binding contributes significantly to these latter values. Fortunately, this nonspecific binding, which we were unable to suppress, is not detected by microcalorimetry. Since the nonspecific binding might somewhat influence the slope of the Scatchard plot of Figure 7, we assume that four rather than five specific Mg^{2+}-binding sites exist in CaM. The specific interaction of Mg^{2+} with CaM is not influenced by substituting NaCl with KCl (Figure 6).

Mg^{2+}–H^+ Antagonism in CaM. In a complementary study to that of the Ca^{2+}–proton antagonism, we monitored proton release upon Mg^{2+} binding at pH 6.0 and 5.0 in a pH-stat assembly (Figure 8) and at pH 5.3 by microcalorimetry in different buffers (Table I). Figure 8 shows that the release of protons follows isotherms with K_{Mg} values of 167 and 72 M^{-1}, respectively. These affinity constants are in the same range as the one found by microcalorimetry, which indicates

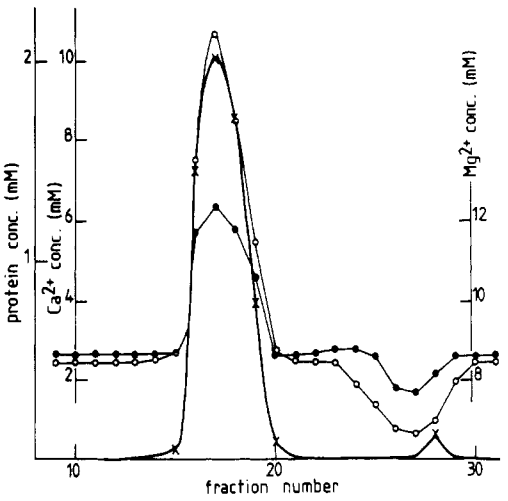

FIGURE 9: Typical elution profile of Sephadex G-25 chromatography in the presence of 9.3 mM $MgCl_2$ and 2.5 mM $CaCl_2$. Fractions of 1 mL were collected. Concentration of CaM (×), Ca^{2+} (○), and Mg^{2+} (●).

that the proton release is identical for each of the Mg^{2+}-binding sites. the same conclusion is reached from Table II, where a K_{Mg} value of 140 M^{-1} provided optimal fitting. The maximal proton release at pH 7.5, 7.0, 6.0, 5.3, and 5.0 amounts to 0.0, 0.07 (Tanokura & Yamada, 1984), 0.66, 2.45, and 5.3 mol·(mol of CaM)$^{-1}$, and the Scatchard plot of these data (not shown) indicates that two protons are release per mole of bound Mg^{2+} from a group with a pK_i around 5.0. Although this study was not completed to the same degree as that of the Ca^{2+}–H^+ antagonism, one can conclude that binding of Mg^{2+} to CaM induces a release of protons from a proton ligand that is different from the one affected by Ca^{2+} binding.

Ca^{2+}–Mg^{2+} Antagonism in CaM. Since CaM appears to possess four binding sites for Ca^{2+} as well as four specific sites for Mg^{2+}, one wonders then whether simple competition exists between the two ions (Haiech et al., 1981; Ogawa & Tanokura, 1984) or a more complex relationship. Therefore the interaction of each of the two ions with CaM was studied in the presence of the other. Figure 1B shows the enthalpy titration profile of Ca^{2+} interaction with CaM in the presence of 30 mM $MgCl_2$. Within experimental errors, the data can be fitted according to eq 3 and 5 of the Appendix with K_{Ca}(app) = 7.2×10^4 M^{-1} and $\Delta H° = -24.0$ kJ·(mol of protein)$^{-1}$. Figure 1B alsc shows that in Tris-HCl buffer the reaction is more exothermic, pointing to a proton release of 0.12 H^+ per mole of CaM; therefore the corrected $\Delta H°$ is −22.6 kJ·mol^{-1}. It should be noted that, according to the affinity constant for Mg^{2+} determined above, the protein was initially only 80% saturated with Mg^{2+} in this experiment. Therefore, K_{Ca} would be lower and $\Delta H°$ more exothermic if the experiment could be carried out in the presence of saturating Mg^{2+} concentrations ([Mg^{2+}] > 0.15 M).

Figure 6 shows the enthalpy titration profile of Mg^{2+} binding to CaM in the presence of 1 mM $CaCl_2$. This reaction is endothermic with a very slow degree of progression; curve fitting of the data according to eq 3 and 5 of the Appendix yields a K_{Mg} of 35 M^{-1} and a $\Delta H°$ of 24.4 kJ·mol^{-1}. The latter value has not to be corrected for proton release since that is negligible (Figure 6, experiment carried out in Tris-HCl buffer). To get an idea about the stoichiometry, direct Mg^{2+}-binding studies were carried out in the presence of saturating Ca^{2+} concentrations ([Ca^{2+}] > $100K_{diss}$). A typical elution profile of simultaneous Ca^{2+} and Mg^{2+} binding to CaM is shown in Figure 9. Table II clearly shows that CaM can bind Mg^{2+} even when Ca^{2+} occupies the four Ca^{2+}-binding sites. The experimental precision is understandably poor but, assuming a K_{Mg} of 35 M^{-1}, the most plausible value for the stoichiometry of Mg^{2+} binding to CaM in the presence of Ca^{2+} is 4, as was found also in the absence of Ca^{2+}.

Table III: Thermodynamic Parameters for Interaction of Ca^{2+} and Mg^{2+} with CaM[a]

interaction	K (M^{-1})	$\Delta G°$ (kJ·mol^{-1})	$\Delta H°$ (kJ·mol^{-1})	$\Delta S°$ (J·K^{-1}·mol^{-1})
CaM + Ca^{2+}	1.05×10^5	−28.7	4.9	113
CaM + Mg^{2+}	140	−12.2	18.2	102
CaM·Ca + Mg^{2+}	35	−8.8	6.1	50
CaM·Mg + Ca^{2+} [b]	2.6×10^4	−25.2 (−27.7)[c]	−7.2 (−5.7)[c]	60

[a] Values are given per metal-binding site assuming four Ca^{2+}- and four Mg^{2+}-binding sites. [b] Calculated from the values of the above reactions assuming Scheme I. [c] Measured at 30 mM free Mg^{2+}, i.e., at an initial Mg^{2+} saturation of 81% and final Mg^{2+} saturation of 51% according to Scheme II and eq 9 and 10 of the Appendix.

General Scheme for Ca^{2+}–Mg^{2+} Antagonism in CaM. Altogether, our data on Ca^{2+}–Mg^{2+}, Ca^{2+}–H^+, and Mg^{2+}–H^+ antagonism suggest that the four Ca^{2+}- and four Mg^{2+}-binding sites in CaM are not exactly the same but influence each other's affinity due to negative free-energy coupling between the sites. The affinity of CaM for Mg^{2+} decreases 4-fold in the presence of millimolar concentrations of Ca^{2+}; the affinity for Ca^{2+} is affected to the same degree in the presence of high concentrations of Mg^{2+}. The most plausible scheme that accounts for all the data is as shown in Scheme II, for each of the four metal-binding domains in CaM. In Scheme II, values for the affinity constants of each equilibrium reaction are good estimates. The concomitant enthalpy and entropy changes are summarized in Table III.

Scheme II

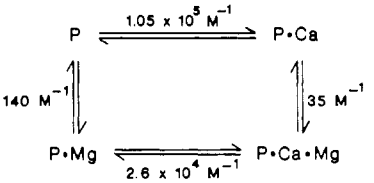

Ca^{2+} binding to CaM is endothermic in the absence of Mg^{2+} but exothermic in the presence of 30 mM Mg^{2+}. It was thus interesting to know the thermal effect of Ca^{2+} binding at physiological concentrations of Mg^{2+}. Figure 10 shows the enthalpy titration profile of Ca^{2+} binding at different concentrations of Mg^{2+}. The reaction enthalpy equals zero at 2 mM free Mg^{2+}, indicating that under physiological conditions binding of Ca^{2+} to CaM is entirely driven by entropy change. The experiment shown in Figure 10 also served as a test of our proposed model of Ca^{2+}–Mg^{2+} antagonism: a reasonably good fit is obtained between the experimental data and the theoretical behavior (solid line) calculated with eq 9 of the Appendix, assuming the theory of negative free-energy coupling between Ca^{2+} and Mg^{2+} binding with the values of the four $\Delta H°$ changes and of the four equilibrium constants proposed above.

Discussion

In light of the controversy about the properties of the four Ca^{2+}-binding domains in CaM (see the introduction), the first aim of this study was to screen for ion-binding characteristics

Table IV: Ca^{2+}- and Putative Mg^{2+}-Binding Sites in the Four Domains of Bovine Brain CaM[a]

		E-helix	Loop	F-helix
			X Y Z -Y -X -Z	
Domain I	(9-42)	I-A-E-F-K-E-A-F-S-L-F-D-K-D-G-D-G-T-I-T-T-K-E-L-G-T-V-M-R-S-L-G-Q-N		
Domain II	(45-78)	E-A-E-L-Q-D-M-I-N-E-V-D-A-D-G-N-G-T-I-D-F-P-E-F-L-T-M-M-A-R-K-M-K-D		
Domain III	(82-115)	E-E-E-I-R-E-A-F-R-V-F-D-K-D-G-N-G-Y-I-S-A-A-E-L-R-H-V-M-T-N-L-G-E-K		
Domain IV	(118-149)	D-E-E-V-D-E-M-I-R-E-A-D-I-D-G-D-G-Q-V-N-Y-E-E-F-V-Q-M-M-T-A-K		

[a] The putative Mg^{2+}-binding residues in each domain are indicated by the two asterisks. The numbers in parentheses correspond to the positions in the complete sequence of CaM. X, Y, and Z indicate the residues involved in Ca^{2+} coordination (Kretsinger, 1979). The sequence was taken from Watterson *et al.* (1980), as modified by Wada *et al.* (1985).

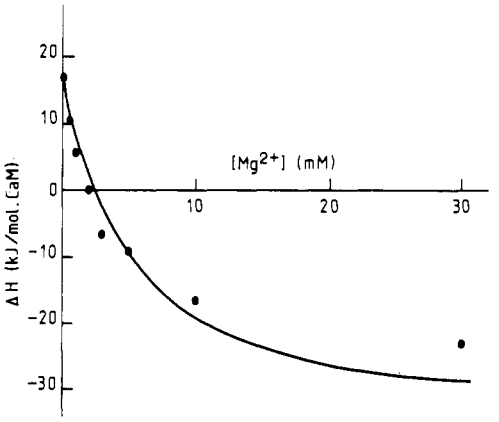

FIGURE 10: Enthalpy change of Ca^{2+} saturation of CaM in the presence of varying concentrations of $MgCl_2$. CaM concentration after mixing was 50 μM. Reaction buffer was 50 M PIPES–NaOH, pH 7.5, 150 mM NaCl, and $MgCl_2$ as indicated on the abscissa. The reaction enthalpy was monitored after 1 mM $CaCl_2$ (concentration before mixing) was mixed in the reaction buffer. The solid line was calculated by assuming that the following reaction takes place: $CaM{\cdot}Mg_x + 4Ca^{2+} \rightarrow CaM{\cdot}Ca_3{\cdot}Mg_y + (x-y)Mg^{2+}$. The values of x and y were calculated with eq 9 of the Appendix by using K_{eq} values presented in Scheme II (Results). The following $\Delta H°$ values (not corrected for proton release and relative to metal-free CaM) were taken: 72.8 kJ·mol^{-1} for $CaM{\cdot}Mg_4$, 17.0 kJ·mol^{-1} for $CaM{\cdot}Ca_4$, and 41.3 kJ·mol^{-1} for $CaM{\cdot}Ca_4{\cdot}Mg_4$.

that discriminate between the two pairs of Ca^{2+}-binding sites, i.e., the pairs located in the N- and the C-terminal half of CaM, respectively. However, our data showed that these four domains not only have identical intrinsic affinity constants—as defined by Kotz and Hunston (1979)—but also an identical enthalpy of 4.9 kJ·(mol of site)$^{-1}$ upon binding of Ca^{2+}. This result is at variance with that of Tanokura and Yamada (1984), who reported two categories of enthalpy change: 1.6 Ca^{2+} bind with $\Delta H° = 3.8$ kJ·(mol of site)$^{-1}$ and 1.4 Ca^{2+} bind with $\Delta H° = 7.4$ kJ·(mol of site)$^{-1}$. Given the too low number of titratable sites, the CaM used in their study may have been partially denatured by the drastic conditions used for metal removal; furthermore, the latter was far from complete. Our data indicate that the two fundamental parameters of Ca^{2+} interaction, $\Delta H°$ and $\Delta S°$, are identical for each Ca^{2+}-binding domain. Furthermore, Mg^{2+} and H^+ antagonize Ca^{2+} binding to each of the four domains to the same degree. The lack of discrimination is illustrated by the following facts: (1) upon a raise of the Mg^{2+} or H^+ concentration the Ca^{2+} binding isotherms are shifted but do not change in shape (Figure 5; Haiech et al., 1981); (2) also, in the presence of high Mg^{2+} concentrations, Ca^{2+} binding to each of the four domains is driven by the same enthalpy change, which now is exothermic (Figure 1; Tanokura & Yamada, 1984;) (3) proton release is identical in each Ca^{2+}-binding step. All these results indicate that Ca^{2+}-binding under normal and perturbing ionic conditions proceeds as if the four domains behave in an identical manner.

In the absence of Ca^{2+}, the chemical group responsible for the Ca^{2+}–H^+ antagonism displays an ionization constant of $10^{6.17}$. The most plausible ligand having such an ionization constant is a pair of carboxyl groups involved in a close carboxyl–carboxylate interaction. Such interactions have been found in many protein structures and are attributed to the sharing of a proton by the two negatively charged side chains (Sawyer & James, 1982). In Ca^{2+}-free CaM, two carboxyl groups would be forced in a restricting, near-neighbor arrangement leading to an anomalous high pK_i. Ca^{2+} binding then disrupts this interaction and may force one or both carboxyl groups to participate in other bonds. In light of a recent report on structure stabilization in the central α-helix of calcium-binding proteins (Sundaralingam et al., 1985), we speculate that the following three pairs would form carboxyl–carboxylate bonds: Asp_{78}–Glu_{82}, Asp_{80}–glu_{83}, and Glu_{84}–Glu_{87}. Indeed, in each of these pairs, one partner at least can alternatively form a salt bridge (in the Ca^{2+}-saturated state): Asp_{78} with Arg_{74}, Asp_{80} with Lys_{77}, Glu_{82} with Arg_{86}, and Glu_{87} with Arg_{90}.

Until now, nearly all the information on the interaction of CaM with Mg^{2+} came from conformational or Ca^{2+}–Mg^{2+} competition studies; detailed direct binding studies were lacking, apparently due to the low affinity of CaM for Mg^{2+}. Indeed, at a free [Mg^{2+}] yielding half-maximal saturation, the concentration of bound Mg^{2+} can only be accurately determined by equilibrium gel filtration or dialysis provided the equilibrated solution contains at least 50 mg of CaM·mL^{-1}. This study showed that microcalorimetry is very well suited for the precise determination of the affinity constant of Mg^{2+} for CaM even in the presence of millimolar Ca^{2+}. Knowledge of the affinity constant (140 M^{-1} in the absence of Ca^{2+}) combined with direct binding data shown that CaM contains four Mg^{2+}-binding sites. In the presence of saturating Ca^{2+} concentrations, the value of K_{Mg} (35 M^{-1}) together with direct binding dat also points to a stoichiometry of four Mg^{2+} per CaM. These data suggest that the Ca^{2+}- and Mg^{2+}-binding sites on CaM are different and that at infinite concentrations of both cations the species $CaM{\cdot}Ca_4{\cdot}Mg_4$ prevails. The values of the enthalpy changes also are in favor of simultaneous Ca^{2+} and Mg^{2+} binding (Table III). The Ca^{2+}- and Mg^{2+}-binding sites are not identical but influence each other: their affinities for the cations are linked by a negative free-energy coupling of 3.4 kJ·site^{-1}, in other words by a 4-fold decrease of the

affinity constants in the presence of infinite concentrations of the antagonistic cation.

As a very preliminary guess on the Mg^{2+}–H^+ antagonism, one would say that two proton ligands with a pK_i of ca 5.0 are involved in the binding of one Mg^{2+} ion. Likely candidates for binding Mg^{2+} in each of the four domains of CaM are proposed in Table IV. The α-carbon atoms of these two amino acids residues are on the same side of the E helices, and the centers of their γ- or δ-carboxyl groups can easily be positioned at about 1.3 Å from each other for the insertion of a Mg^{2+} ion. Such imposed close contact between two carboxyl groups is also present in malonic acid and cyclobutane-1,1-dicarboxylic acid, which display pK_i values of 5.28 and 5.22, respectively, and a K_{Mg} of 129 M^{-1} (Martell & Smith, 1977b). Interestingly, the putative Mg^{2+}-binding amino acid residues are very well conserved in the four domains of all calmodulins, in some domains of troponin C, and in different regulatory light chains of myosin, where small Mg^{2+} effects upon Ca^{2+} binding have been reported, but not in parvalbumins and invertebrate sarcoplasmic Ca^{2+}-binding proteins, where Mg^{2+} strongly affects the Ca^{2+}-binding properties.

The fundamental parameters of Ca^{2+} binding to CaM do not resemble those of other proteins with a rather high affinity for Ca^{2+} ($K \geq 10^5$ M^{-1}). In CaM, the reaction is entirely entropy driven with a small endothermic component (this study; Tanokura & Yamada, 1984). In troponin C, Ca^{2+} binding to the so-called specific sites is entirely enthalpy driven with no change in entropy (Potter et al., 1977). Ca^{2+} binding to the Ca^{2+}–Mg^{2+} sites of the latter protein and also to parvalbumins is both enthalpy and entropy driven (Potter et al., 1977; Moeschler et al., 1980; Tanokura & Yamada, 1984). Finally in α-lactalbumin, Ca^{2+} binding is so strongly enthalpy driven that a large negative entropy component accompanies the reaction (Van Ceunebroeck et al., 1985; Schaer et al., 1985). Although there are many structural homologies between the Ca^{2+}-binding domains of these proteins (except that of α-lactalbumin), the fundamental differences shown above may be responsible for their very specific functions in the cell.

Acknowledgments

We thank Professor D. Janjic for his interest and help throughout this work and Catherine Zurcher for skillful technical assistance.

Appendix

Determination of Affinity Constants and Maximal Signal Change of the Interaction of Divalent Cations with CaM. Assuming identical affinity constants (K) for the Ca^{2+}- and Mg^{2+}-binding sites on CaM (model 1), the interaction of these divalent metal ions with the protein can be described with reference to one site (S) rather than to the whole protein:

$$S + M^{2+} \rightleftarrows S{\cdot}M \quad (1)$$

with

$$K = \frac{[S{\cdot}M]}{([M_T] - [S{\cdot}M])([S_T] - [S{\cdot}M])} = \frac{\nu}{([M_T] - [S_T]\nu)(1 - \nu)} \quad (2)$$

where $[S_T]$ and $[M_T]$ are the total concentrations of metal-binding site and of metal, respectively, and ν is the fractional saturation, equals $[S{\cdot}M]/[S_T]$.

Equation 2 can be solved for ν to yield a quadratic equation with the following root [see also Richards and Vithayathil (1959)]:

$$\nu = \{1 + K[S_T] + K[M_T] - [(1 + K[S_T] + K[M_T])^2 - 4K^2[S_T][M_T]]^{1/2}\}/\{2K[S_T]\} \quad (3)$$

Assuming two pairs of metal-binding sites of different affinities (model 2, with $K = K_1$ or K_2 for S_{1T} and S_{2T}, respectively), the overall fractional saturation

$$\bar{\nu} = (\nu_1 + \nu_2)/2 \quad (4)$$

where ν_1 and ν_2 each were calculated by eq 3.

The experimentally determined signal change, ΔY_{exptl} (corresponding in this work either to a heat exchange or to a proton release), as a function of $[M_T]$ can adequately be described by eq 3 or 4, since

$$\Delta Y_{exptl} = 4\nu\Delta Y_{max} \text{ (model 1) or } \Delta Y_{exptl} = 4\bar{\nu}\Delta Y_{max} \text{ (model 2)} \quad (5)$$

where ΔY_{max} is the overall change per mole of CaM. The experimental data ΔY_{exptl} vs. $[M_T]$ (n experiments) were analyzed according to eq 3 and 5 by iteratively varying K and ΔY_{max}: a minimum in the function $\sum_{i=1}^{i=n}(\Delta Y_{exptl} - \Delta Y_{calcd})^2$ yields the best fitting values for K and ΔY_{max}. In some experiments, the data were analyzed iteratively according to eq 4 and 5 by imposing a difference of 1 order between K_1 and K_2. All the iterative analyses were carried out with a MINUITS routine from the CERN library (Geneva).

Determination of Fraction of Bound Ligand A or B in a Free-Energy-Coupled System Involving CaM and Two Ligands. In Scheme I (Materials and Methods), the fraction of bound A per site is given by

$$\text{bound A/site} = ([S{\cdot}A] + [S{\cdot}A{\cdot}B])/[S_T] \quad (6)$$

where $[S_T]$ is the total concentration of metal-binding sites. From the rule of energy conservation, i.e., $[S_T] = [S] + [S{\cdot}A] + [S{\cdot}B] + [S{\cdot}A{\cdot}B]$, it can be deduced that

$$[S{\cdot}A] = [S_T]/[1 + (K_a[A])^{-1} + K_b[B](K_a[A])^{-1} + K_b^a[B]] \quad (7)$$

and

$$[S{\cdot}A{\cdot}B] = [S_T]/[1 + (K_a^b[A])^{-1} + (K_b^a[B])^{-1} + [A][B](K_aK_b^a)^{-1}] \quad (8)$$

Since $K_aK_b^a = K_bK_a^b$, eq 5–7 can be reduced to [see also Cox et al. (1982)]

$$\text{bound A/site} = \frac{1 + (K_b^a[B])^{-1}}{1 + (K_a^b[A])^{-1} + (1 + K_a[A])^{-1}(K_b^a[B])^{-1}} \quad (9)$$

Similarly

$$\text{bound B/site} = \frac{1 + (K_a^b[A])^{-1}}{1 + (K_b^a[B])^{-1} + [1 + (K_b[B])^{-1}](K_a^b[A])^{-1}} \quad (10)$$

Registry No. Ca, 7440-70-2; H^+, 12408-02-5; Mg, 7439-95-4.

References

Andersson, T., Drakenberg, T., Forsén, S., & Thulin, E. (1982) *Eur. J. Biochem. 126*, 501–505.

Bayley, P. M., Ahlström, P., Martin, S. R., & Forsén, S. (1984) *Biochem. Biophys. Res. Commun. 120*, 185–191.

Beres, L., & Sturtevant, J. M. (1971) *Biochemistry 10*, 2120–2125.

Burger, D., Stein, E. A., & Cox, J. A. (1983) *J. Biol. Chem. 258*, 14733–14739.

Burger, D., Cox, J. A., Comte, M., & Stein, E. A. (1984)

Biochemistry 23, 1966–1971.
Cox, J. A. (1984) *Fed. Proc., Fed. Am. Soc. Exp. Biol. 43*, 3000–3004.
Cox, J. A., Malnoë, A., & Stein, E. A. (1981) *J. Biol. Chem. 256*, 3218–3222.
Cox, J. A., Comte, M., & Stein, E. A. (1982) *Proc. Natl. Acad. Sci. U.S.A. 79*, 4265–4269.
Cox, J. A., Comte, M., Malnoë, A., Burger, D., & Stein, E. A. (1984) *Met. Ions Biol. Syst. 17*, 215–293.
Debye, P., & Hückel, E. (1923) *Phys. Z. 24*, 185–208.
Gopalakrishna, R., & Anderson, W. B. (1982) *Biochem. Biophys. Res. Commun. 104*, 830–836.
Haiech, J., Klee, C. B., & Demaille, J. G. (1981) *Biochemistry 20*, 3890–3897.
Klotz, I. M., & Hunston, D. L. (1979) *Arch. Biochem. Biophys. 193*, 314–328.
Kretsinger, R. H. (1979) *Adv. Cyclic Nucleotide Res. 11*, 2–26.
Martell, A. E., & Smith, R. M. (1974) in *Critical Stability Constants*, Vol. 1, pp 61–62, Plenum, New York and London.
Martell, A. E., & Smith, R. M. (1977a) in *Critical Stability Constants*, Vol. 3, pp 3–7, Plenum, New York and London.
Martell, A. E., & Smith, R. M. (1977b) in *Critical Stability Constants*, Vol. 3, pp 95–107, Plenum, New York and London.
Martin, S. R., Andersson Teleman, A., Bayley, P. M., Drakenberg, T., & Forsén, S. (1985) *Eur. J. Biochem. 151*, 543–550.
Minowa, O., & Yagi, K. (1984) *J. Biochem. (Tokyo) 96*, 1175–1182.
Moeschler, J. H., Schaer, J. J., & Cox, J. A. (1980) *Eur. J. Biochem. 111*, 73–78.
Ogawa, Y., & Tanokura, M. (1984) *J. Biochem. (Tokyo) 95*, 19–28.
Potter, J. D., Hsu, F. J., & Pownall, J. H. (1977) *J. Biol. Chem. 252*, 2452–2454.
Potter, J. D., Strang-Brown, P., Walker, P. L., & Iida, S. (1983) *Methods Enzymol. 102*, 135–143.
Richards, F. M., & Vithayathil, P. J. (1959) *J. Biol. Chem. 243*, 1459–1465.
Sawyer, L., & James, M. N. G. (1982) *Nature (London) 295*, 79–80.
Schaer, J. J., Milos, M., & Cox, J. A. (1985) *FEBS Lett. 190*, 77–80.
Sundaralingam, M., Drendel, W., & Greaser, M. (1985) *Proc. Natl. Acad. Sci. U.S.A. 82*, 7944–7947.
Tanokura, M., & Yamada, K. (1984) *J. Biochem. (Tokyo) 95*, 643–649.
Van Ceunebroeck, J. C., Hanssens, I., Joniau, M., & Van Cauwelaert, F. (1985) *J. Biol. Chem. 260*, 10944–10947.
Wada, Y., Sobue, K., Morimoto, K., Matsuo, T., Katakuse, I., Kakiuchi, S., Matsuda, H., & Hayashi, A. (1985) *Biochim. Biophys. Acta 832*, 383–386.
Wallace, R. W., & Cheung, W. Y. (1979) *J. Biol. Chem. 254*, 6564–6571.
Wang, C. L. A. (1985) *Biochem. Biophys. Res. Commun. 130*, 426–430.
Watterson, D. M., Sharief, F., & Vanaman, T. C. (1980) *J. Biol. Chem. 255*, 962–975.

Amine Uptake into Intact Mast Cell Granules in Vitro†

Russell I. Ludowyke and David Lagunoff*

Department of Pathology, St. Louis University School of Medicine, St. Louis, Missouri 63104

Received February 7, 1986; Revised Manuscript Received June 27, 1986

ABSTRACT: Histamine, the principal amine of rat peritoneal mast cells, is taken up into isolated granules with intact membranes. Uptake is pH- and concentration-dependent and is not stimulated by the addition of Mg^{2+}-ATP. The saturable uptake has a K_m of 91.1 μM and a V_{max} of 95.4 pmol (mg of protein)$^{-1}$ min^{-1}. Uptake is abolished by 5 mM ammonium ion. 5-HT, the other endogenous amine of the granules, and dopamine and tyramine, which do not occur naturally in rat mast cells, each competitively inhibits [^{3}H]-histamine uptake with K_i's close to 1 μM. Reserpine, a putative amine carrier blocker, inhibits uptake at nanomolar concentrations. At high concentrations, uptake of [^{3}H]-5-HT is nonsaturable; at low concentrations, a saturable component is observed with a K_m of 1.6 μM. Uptake of [^{3}H]-5-HT is not enhanced by Mg^{2+}-ATP. It is pH-dependent but with a lower apparent pK_a than that of histamine. [^{3}H]-5-HT uptake can be completely inhibited by ammonium ions. Amine inhibition of [^{3}H]-5-HT uptake gives nonlinear Dixon plots, and high concentrations of the competing amines or reserpine cannot completely block uptake. We propose a model consistent with these results in which amine uptake occurs by several distinct saturable transport systems. According to the model, histamine is transported by a single system, which also transports 5-HT and dopamine. 5-HT and dopamine are transported by one or more other systems.

Connective tissue mast cells of the rat contain histamine and 5-HT. These amines, located in the cell's specific granules, are secreted exocytotically and coordinately in response to a variety of agents (Lagunoff et al., 1983).

The mechanism by which amines enter secretory granules, though unexplored for mast cell granules, has been previously studied in chromaffin granules and platelet-dense granules. Current evidence suggests that a Mg-dependent ATPase, present in the chromaffin and the dense granule membrane, creates an electrochemical gradient comprised of both a pH

† This work was supported in part by NIH Grant HL 25402.

0006-2960/86/0425-6287$01.50/0